

# Low-mass X-ray binaries indicate a top-heavy stellar initial mass function in ultra compact dwarf galaxies

Jörg Dabringhausen<sup>1</sup>, Pavel Kroupa<sup>1</sup>, Jan Pflamm-Altenburg<sup>1</sup> and Steffen Mieske<sup>2</sup>

<sup>1</sup>*Argelander-Institut für Astronomie (AIfA), Auf dem Hügel 71, 53121 Bonn, Germany*

<sup>2</sup>*European Southern Observatory, Alonso de Cordova 3107, Vitacura, Santiago, Chile*

joedab@astro.uni-bonn.de, pavel@astro.uni-bonn.de,  
jpflamm@astro.uni-bonn.de, smieske@eso.org

## ABSTRACT

It has been shown before that the high mass-to-light ratios of ultra compact dwarf galaxies (UCDs) can be explained if their stellar initial mass function (IMF) was top-heavy, i.e. that the IMF was skewed towards high mass stars. In this case, neutron stars and black holes would provide unseen mass in the UCDs. In order to test this scenario with an independent method, we use data on which fraction of UCDs has a bright X-ray source. These X-ray sources are interpreted as low-mass X-ray binaries (LMXBs), i.e. binaries where a neutron star accretes matter from an evolving low-mass star. We find that LMXBs are indeed up to 10 times more frequent in UCDs than expected if the IMF was invariant. The top-heavy IMF required to account for this overabundance is the same as needed to explain the unusually high mass-to-light ratios of UCDs and a top-heavy IMF appears to be the only simultaneous explanation for both findings. Furthermore, we show that the high rate of type II supernovae (SNII) in the star-burst galaxy Arp 220 suggests a top-heavy IMF in that system. This finding is consistent with the notion that star-burst galaxies are sites where UCDs are likely to be formed and that the IMF of UCDs is top-heavy. It is estimated that the IMF becomes top-heavy whenever the star formation rate per volume surpasses  $0.1 \text{ M}_{\odot} \text{ yr}^{-1} \text{ pc}^{-3}$  in pc-scale regions.

*Subject headings:* galaxies: dwarf — galaxies: star burst — galaxies: stellar content — stars: mass function, luminosity function — stars: neutron

## 1. Introduction

The stellar initial mass function (IMF) quantifies the distribution of stellar masses in a newly born stellar population. Together with the dependency of stellar evolution on stellar mass and metallicity, as well as the rate at which stars are formed in the Universe, the shape of the IMF determines the chemical evolution of the Universe and how its stellar content changes with time. The shape of the IMF also has important implications for the evolution of star clusters. Thus, knowing the shape of the IMF is crucial for a broad variety of astrophysical problems.

Resolved stellar populations in the Milky Way and its satellites support the notion that the IMF

does not depend on the conditions under which star formation takes place, but that the stellar masses are distributed according to a single IMF known as the *canonical* IMF (Kroupa 2001, 2002; Kumar et al. 2008; Bastian et al. 2010). Ultra compact dwarf galaxies (UCDs) on the other hand provide evidence for the opposite notion, namely that the IMF varies and is top-heavy.

These UCDs are stellar systems that have first been discovered in the Fornax galaxy cluster (Hilker et al. 1999). They have *V*-band luminosities between  $10^6$  and some  $10^7 \text{ L}_{\odot}$ , but half-light radii of only about 50 pc or less (Drinkwater et al. 2003; Mieske et al. 2008). The confirmed UCDs are at distances where they cannot be resolved into stars with current telescopes, but constrains on

their stellar populations can be set by quantities derived from their integrated spectra. One such quantity are the dynamical mass-to-light ( $M/L$ ) ratios of UCDs, i.e. mass estimates based on the density profile and the internal velocity dispersion of the UCDs (Hasegan et al. 2005; Hilker et al. 2007; Evstigneeva et al. 2007; Mieske et al. 2008). For a clear majority of the UCDs, the  $M/L$  ratios derived from their dynamics are higher than it would be expected if they were pure stellar populations that formed with the canonical IMF (Hasegan et al. 2005; Dabringhausen et al. 2008; Mieske et al. 2008). This has been taken as evidence for an IMF skewed towards high-mass stars (Dabringhausen et al. 2009), i.e. a top-heavy IMF. The elevated  $M/L$  ratios of UCDs would then be explained by a large population of neutron stars and black holes (hereafter called dark remnants), because the age of the UCDs (Evstigneeva et al. 2007; Chilingarian et al. 2008) implies that all massive stars in them have completed their evolution.

It is plausible that the IMF in UCDs is skewed towards high-mass stars. Molecular clouds massive enough to be the progenitors of UCDs become impenetrable for far-infrared radiation while they collapse and become a UCD-type star-cluster. Internal heating of the molecular cloud leads to a higher Jeans-mass in them preferring the formation of high-mass stars (Murray 2009). A molecular cloud can also be heated by an external flux of highly energetic cosmic rays originating from a local overabundance of type II supernovae increasing the local Jeans-mass (Papadopoulos 2010). With the young UCDs being very compact, also crowding of proto-stellar cores and their subsequent merging in young UCDs may lead to an overabundance of high-mass stars in them (Dabringhausen et al. 2010; Weidner et al. 2011).

However, the high  $M/L$  ratios of UCDs could in principle also be due to non-baryonic dark matter (DM), as was suggested by Goerdt et al. (2008) and Baumgardt & Mieske (2008). This is because dark remnants and non-baryonic DM would have the same effect on the  $M/L$  ratios of the UCDs, provided that a large enough amount of non-baryonic DM can gather within the UCDs. Note that that non-baryonic DM is an unlikely cause for the high  $M/L$  ratios of UCDs, since non-baryonic

DM is predicted to gather on rather large scales while UCDs are very compact (Gilmore et al. 2007; Murray 2009). However, in order to exclude this possibility completely, the presence of a sufficient number of dark remnants has to be confirmed independently by a method that does not rely on the fact that dark remnants are non-luminous matter like non-baryonic DM.

Such a method is searching for low-mass X-ray binaries (LMXBs) in UCDs. In these binary systems, a dark remnant and an evolving low-mass star are orbiting around each other. The expanding outer atmosphere of the low-mass companion is accreted by the dark remnant. This matter produces a characteristic X-ray signature. The number of LMXBs depends on the number of NSs and stellar-mass black holes (BHs) and thus on the IMF (Verbunt & Hut 1987; Verbunt 2003). This implies that stellar systems with a top-heavy IMF can be distinguished from stellar systems with the canonical IMF by an excess of LMXBs.

The formulation of the IMF that is used throughout this paper is introduced in Sec. (2). In Sec. (3), the LMXB-abundance in globular clusters (GCs) and UCDs in dependency of the IMF and this model is compared to observations. The type-II supernova rate in star-bursting galaxies in dependency of the top-heaviness of the IMF is discussed in Sec. (4). It is found in Sec. (3) and Sec. (4), respectively, that the UCDs and the star-bursting galaxy Arp 220 show indications for a top-heavy IMF. This suggests that the star formation rate per volume is perhaps the parameter that determines whether the IMF in that volume becomes top-heavy, as is argued in Sec. (5). Conclusions are given in Sec. (6).

## 2. The initial stellar mass function

A varying IMF can be formulated as

$$\xi(m) = k k_i m^{-\alpha_i}, \quad (1)$$

with

$$\begin{aligned} \alpha_1 &= 1.3, & 0.1 \leq \frac{m}{M_\odot} < 0.5, \\ \alpha_2 &= 2.3, & 0.5 \leq \frac{m}{M_\odot} < m_{\text{tr}}, \\ \alpha_3 &\in \mathbb{R}, & m_{\text{tr}} \leq \frac{m}{M_\odot} \leq m_{\text{max}}, \end{aligned}$$

where  $m$  is the initial stellar mass, the factors  $k_i$  ensure that the IMF is continuous where the power changes and  $k$  is a normalization constant.  $\xi(m)$  equals 0 if  $m < 0.1 M_\odot$  or  $m > m_{\max}$ , where  $m_{\max}$  is a function of the star-cluster mass (Weidner & Kroupa 2006; Weidner et al. 2010) and  $m_{\text{tr}}$  is the stellar mass at which the IMF begins to deviate from the canonical IMF. For  $m_{\text{tr}} = 1 M_\odot$ , the formulation of the IMF used here is identical with the one used in Dabringhausen et al. (2009), so that results found here for this choice of  $m_{\text{tr}}$  can be compared to results in Dabringhausen et al. (2009). For  $\alpha_3 = \alpha_2 = 2.3$ , Equation (1) is the canonical IMF (Kroupa 2001, 2002). For  $\alpha_3 < 2.3$ , the IMF is top-heavy, implying more intermediate-mass stars and in particular more high-mass stars.

In the mass range of UCDs,  $m_{\max}$  is not set by the mass of the stellar system, but by the observed mass limit for stars,  $m_{\max*}$ . Thus,  $m_{\max} = m_{\max*}$  for all UCDs. The actual value of  $m_{\max*}$  is, however, rather uncertain: Estimates range from the canonical value  $m_{\max*} \approx 150 M_\odot$  (Weidner & Kroupa 2004; Oey & Clarke 2005) to  $m_{\max*} \approx 300 M_\odot$  (Crowther et al. 2010, but see Banerjee et al. 2011). In this paper,  $m_{\max*} = 150 M_\odot$  is assumed, but note that assuming  $m_{\max*} = 300 M_\odot$  instead would have little effect on the results reported here (see Section 3.3 and Figure 7).

In the case of GCs and UCDs with LMXBs (see Section 3), the observed luminosity,  $L$ , is known to originate from stars with masses  $m \lesssim 1 M_\odot$ . This is because their stellar populations are old (Evstigneeva et al. 2007; Chilingarian et al. 2008) and the more massive stars have already completed their evolution. Being fixed by observations,  $L$  should however not be changed when the IMF is varied. For the IMF given by Equation (1), this can be achieved by finding  $k$  from the condition

$$\int_{0.1 M_\odot}^{m_{\max*}} \xi_{\text{can}}(m) m dm = 1 M_\odot, \quad (2)$$

where  $\xi_{\text{can}}$  is the canonical IMF, i.e.  $\alpha_3 = 2.3$ . With this normalization, the number density of stars with  $m < 1 M_\odot$  is the same for all values of  $\alpha_3$ , since the normalization is set by the canonical IMF and is therefore not affected by variations of  $\alpha_3$ .

In the case of the SN-rate of Arp 220 (see Sec-

tion 4), the light used to estimate the star formation rate (SFR), i.e. the mass of the material converted into stars per time-unit, originates from stars over the whole range of stellar masses. With the SFR thereby given, we then normalize the IMF such that the SFR remains constant when the IMF is varied. For the IMF given by Equation (1), this can be achieved by finding  $k$  from the condition

$$\int_{0.1 M_\odot}^{m_{\max*}} \xi(m) m dm = 1 M_\odot. \quad (3)$$

With this normalization, the number density of stars with  $m < 1 M_\odot$  decreases with decreasing values of  $\alpha_3$ , i.e. with increasing top-heaviness of the IMF.

Stellar evolution and dynamical evolution turn the IMF of a star cluster into a (time-dependent) mass function of stars and stellar remnants; the star and stellar remnant mass function, SRMF. For a single-age stellar population, the connection between the IMF and the SRMF can be quantified by an initial-to-final mass relation for stars,  $m_{\text{rem}}$ , which can be written as

$$m_{\text{rem}} = \begin{cases} \frac{m}{M_\odot}, & \frac{m}{M_\odot} < \frac{m_{\text{to}}}{M_\odot}, \\ 0.109 \frac{m}{M_\odot} + 0.394, & \frac{m_{\text{to}}}{M_\odot} \leq \frac{m}{M_\odot} < 8, \\ 1.35, & 8 \leq \frac{m}{M_\odot} < 25, \\ 0.1 \frac{m}{M_\odot}, & 25 \leq \frac{m}{M_\odot} \leq m_{\max*}, \end{cases} \quad (4)$$

where  $m_{\text{to}}$  is the mass at which stars evolve away from the main sequence at a given age (Dabringhausen et al. 2009). UCDs typically have ages of  $\approx 10$  Gyr (Evstigneeva et al. 2007; Chilingarian et al. 2008), which implies  $m_{\text{to}} \approx 1 M_\odot$  for them. In the present paper, Equation (4) is used to calculate how the mass of a modeled UCD depends on the variation of its IMF (see Section 3.2.3).

Note that Equation (4) reflects the evolution of single stars. In a binary system, the initial mass of a star that evolves into a black hole is expected to be higher, so that stars with masses up to  $40 M_\odot$  may become NSs instead of BHs (cf. Brown et al. 2001). It is however of minor importance in this paper whether a massive remnant is a NS or a BH. Both kinds of objects can become

bright X-ray sources by accreting matter from a companion star and BHs in such binary systems are actually detected by excluding that they are NSs due to their mass (Casares 2007). Also the total mass of a GC or UCD is not strongly affected by the mass-limit between NSs and BHs. Using Equation (refeq:IMF) with  $m_{\text{tr}} = 1 M_{\odot}$  and Equation (4) with  $m_{\text{to}} = 1 M_{\odot}$ , the total mass of NSs and BHs is 4.2 per cent of the total mass of the stellar system for  $\alpha_3 = 2.3$  (canonical IMF) and 79.9 per cent for  $\alpha_3 = 1$ . These numbers are altered to 3.8 per cent of the total mass of the stellar system for  $\alpha_3 = 2.3$  and 75.0 per cent for  $\alpha_3 = 1$  if the transition from NSs to BHs is shifted from  $25 M_{\odot}$  to  $40 M_{\odot}$ .

### 3. The LMXB-abundance in GCs and UCDs

#### 3.1. Some properties of GCs and UCDs

For a number of GCs and UCDs, data (Mieske et al. 2008) on  $V$ -band luminosity ( $L_V$ ), dynamical mass ( $M_{\text{dyn}}$ ) and effective half-light radius ( $r_h$ ) are available. These data suggest a transition at  $L_V \approx 10^6 L_{\odot}$ , since the  $r_h$  and dynamical  $M/L$  ratios of objects with  $L_V < 10^6 L_{\odot}$  appear to be independent of  $L_V$ , in contrast to objects with  $L_V > 10^6 L_{\odot}$  (see Figures 1 and 2). This motivates to consider the objects with  $L_V < 10^6 L_{\odot}$  as GCs and those with  $L_V \geq 10^6 L_{\odot}$  as UCDs, even though stellar systems close to this transition could be assigned to either one of these classes (Mieske et al. 2008).

Knowing  $r_h$  and  $M_{\text{dyn}}$  of a stellar system allows to estimate its median two-body relaxation time (Spitzer 1987), using

$$t_{\text{rh}} = \frac{0.234}{\log_{10}(M_{\text{dyn}}/M_{\odot})} \times \sqrt{\frac{M_{\text{dyn}} r_h^3}{G}}, \quad (5)$$

where  $G$  is the gravitational constant (Dabringhausen et al. 2008). The significance of  $t_{\text{rh}}$  lies in the fact that it sets the time-scale on which the structure of a self-bound stellar system is changed by the process of energy equipartition. If  $\tau \gtrsim t_{\text{rh}}$  holds for a stellar system with  $\tau$  being its age, it can be considered nearly unaffected by dynamical evolution and is thus only subject to stellar evolution. This is the case for UCDs, as  $t_{\text{rh}} \gtrsim \tau_{\text{H}}$  is valid for them, where  $\tau_{\text{H}}$  is the age of the Universe suggested by

the  $\Lambda$ CDM-model (see Figure 3). Thus, the properties of UCDs can be calculated from their IMF while considering the effects of stellar evolution, but without accounting for the effects of dynamical evolution. This means in particular that the SRMF of UCDs can be calculated from their IMF and Equation (4). Note that GCs, on the other hand, are subject to dynamical evolution, since their ages,  $\tau_{\text{GC}}$  are also similar to  $\tau_{\text{H}}$  and thus  $\tau_{\text{GC}} > t_{\text{rh}}$ .

The data (Mieske et al. 2008) on  $L_V$  and  $r_h$  of individual GCs in the MW and in Centaurus A and UCDs in the Virgo-cluster are also useful for estimating an average  $r_h$ ,  $\bar{r}_h$ , as a function of  $L_V$ . GCs over the luminosity range from  $10^4 L_{\odot}$  to  $10^6 L_{\odot}$  do not show a luminosity-radius trend (McLaughlin 2000; Jordán et al. 2005). The logarithmic average  $r_h$  of GC is

$$\log_{10} \left( \frac{\bar{r}_h}{\text{pc}} \right) = 0.4314 \quad (6)$$

(Jordán et al. 2005). Performing a linear least-squares fit to data in Mieske et al. (2008) on UCDs in the Virgo cluster leads to

$$\log_{10} \left( \frac{\bar{r}_h}{\text{pc}} \right) = 1.076 \log_{10} \left( \frac{L_V}{10^6 L_{V,\odot}} \right) + 0.4314. \quad (7)$$

Note that equality between Equations (6) and (7) at  $L_V = 10^6 L_{\odot}$  was imposed as a secondary condition on the fit of Equation (7) to the data. This secondary condition reflects the fact that the  $r_h$  of GCs are indistinguishable from those of UCDs at  $L \approx 10^6 L_{\odot}$  (see Figures 1 and 2).

#### 3.2. Modeling the LMXB-abundance in GCs and UCDs

##### 3.2.1. The origin of LMXBs in GCs and UCDs

Tight binaries consisting of a dark remnant and a low-mass companion can have in principle two different origins:

1. They can be primordial. In this case a tight binary of a high-mass star and a low-mass star have formed already in the star forming event. The high-mass star explodes in a supernova after a few million years leaving behind a dark remnant which can remain bound to its low-mass companion.

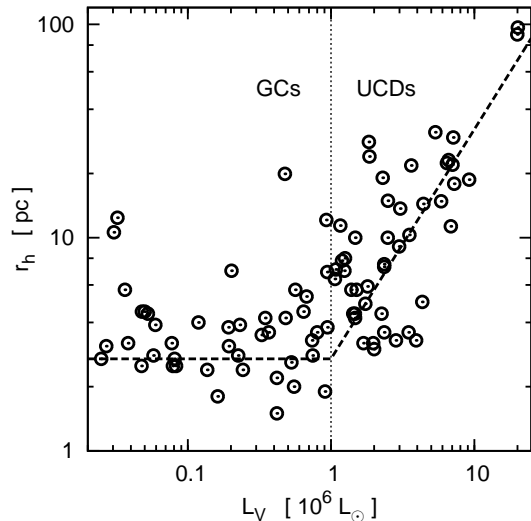


Fig. 1.— The effective half-light radii,  $r_h$ , of GCs and UCDs. The circles show the sample of individual GCs and UCDs from the compilation of Mieske et al. (2008). The dashed line is an estimate of the average  $r_h$  of GCs and UCDs (cf. Equations 6 and 7). The vertical dotted line sets the limit between objects that are considered as GCs and objects that are considered as UCDs. Note that the average  $r_h$  indicated for GCs by the dashed line is lower than the average  $r_h$  of the GCs shown in this figure. This is because the GCs shown here are mostly GCs of the Milky Way while the dashed line corresponds to the average  $r_h$  of GCs in the Virgo-cluster. The GCs in the Virgo cluster tend to be more compact than those around the Milky Way.

2. They have formed through encounters. GCs and UCDs are regions of enormously high stellar density ranging from  $10 \text{ M}_\odot \text{ pc}^{-3}$  to  $10^4 \text{ M}_\odot \text{ pc}^{-3}$  (Dabringhausen et al. 2008). Encounters between dark remnants and low-mass stars are therefore frequent and can lead to the formation of LMXBs due to tidal capture (Verbunt & Hut 1987; Verbunt 2003).

As these formation mechanisms are quite different it is expected that both processes would contribute differently to the LMXB content in GCs and UCDs.

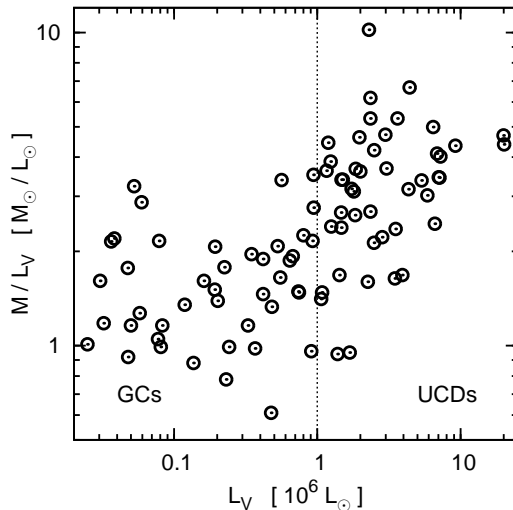


Fig. 2.— The mass-to-light ratios ( $M/L$  ratios) of GCs and UCDs. The circles show the sample of individual GCs and UCDs from the compilation of Mieske et al. (2008). The vertical dotted line sets the limit between objects that are considered as GCs and objects that are considered as UCDs.

There are however strong arguments against a significant contribution from primordial binaries to the LMXB content of GCs and UCDs:

1. The number of LMXBs in GCs is strongly correlated with the encounter rate and thus clearly linked to it (Jordán et al. 2005; Sivakoff et al. 2007).
2. There are several hundred times more LMXBs per unit mass in GCs than in the Galactic field (Verbunt & Hut 1987). The LMXBs in the Galactic field are LMXBs that probably evolved from primordial binaries, since they are in a low-density environment where encounters play no role and most probably formed in star clusters from which they were subsequently ejected. The strong excess of LMXBs in GCs therefore suggests that most LMXBs in GCs form through encounters (Verbunt & Hut 1987).

The number of encounters relevant for the creation of LMXBs, i.e. encounters where a NS can capture a low-mass star (Verbunt & Hut 1987),

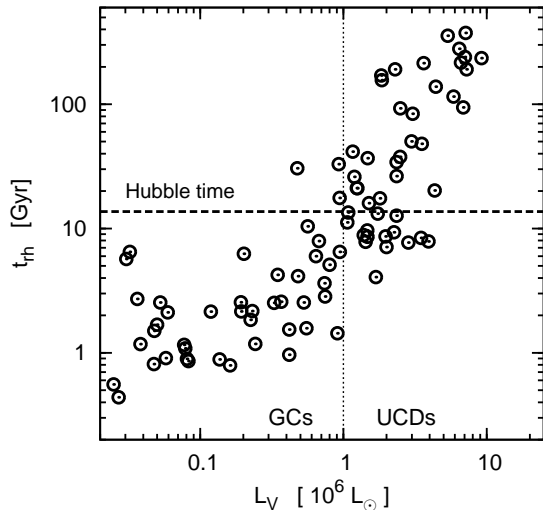


Fig. 3.— The median two-body relaxation times,  $t_{\text{rh}}$ , of GCs and UCDs. The circles show the sample of individual GCs and UCDs from the compilation of Mieske et al. (2008). The dashed horizontal line indicates the age of the Universe,  $\tau_{\text{H}}$ , according to the  $\Lambda$ CDM-model. The vertical dotted line sets the limit between objects that are considered as GCs and objects that are considered as UCDs. Note that  $t_{\text{rh}} \gtrsim \tau_{\text{H}}$  for UCDs. Thus, UCDs can be considered dynamically unevolved (Dabringhausen et al. 2008) and they may therefore be considered as galaxies from a stellar dynamical point of view (Forbes & Kroupa 2011).

can be written as

$$\Gamma \propto \frac{n_{\text{ns}} n_{\text{s}} r_{\text{c}}^3}{\sigma}, \quad (8)$$

where  $n_{\text{ns}}$  is the number density of NSs,  $n_{\text{s}}$  is the number density of potential low-mass companion stars,  $r_{\text{c}}$  is the core radius of the stellar system and  $\sigma$  is the velocity dispersion (Verbunt 2003). The potential companions to a NS in a bright LMXB are stars that come from a rather narrow mass range where stars of a given age leave the main-sequence. At this stage of their evolution, the stars expand rapidly, which makes a high accretion rate on the NS possible, which in turn leads to a high X-ray luminosity.

A more recent study by Ivanova et al. (2008) revealed that tidal capture is not the only dynamical process relevant for the formation of LMXBs. Other dynamical processes like direct collisions be-

tween NSs and red giant stars or interactions between stars and existing binaries also play a role and can actually be even more important than tidal captures. However, this does not change the observational finding that the number of LMXBs in GCs scales with  $\Gamma$  (e.g. Jordán et al. 2005). Therefore,  $\Gamma$  seems to be an adequate measure for the stellar dynamical processes that produce LMXBs in general. It is moreover argued in Ivanova et al. (2008) that primordial binaries only make a small contribution to the total population of LMXBs in old GCs.

There are thus strong observational and theoretical motivations for the usage of  $\Gamma$  as a measure for how many LMXBs are expected in GCs and UCDs.

### 3.2.2. The encounter rate in GCs and UCDs for an invariant SRMF

If only a *single*, invariant mass function for stars and stellar remnants (SRMF) is considered for all stellar systems, then

$$n_{\text{ns}} \propto n_{\text{s}} \propto \rho_0 \quad (9)$$

holds, where  $\rho_0$  is the central mass density. Equation (8) can then be rewritten as

$$\Gamma \propto \frac{\rho_0^2 r_{\text{c}}^3}{\sigma} \quad (10)$$

by using Equation (9).

In order to link the theory on LMXB-formation to the optical properties of observed stellar systems, it is in the following assumed that the mass density of a stellar system follows its luminosity density. The structural parameters derived from the distribution of the light in the stellar system can then be translated directly into statements on the distribution of its mass, i.e. quantities that determine the dynamics of the stellar system.

However,  $r_{\text{c}}$  is difficult to measure for GCs and UCDs at the distance of the Virgo cluster, as these stellar systems are barely resolved with current instruments. The projected half-light radius  $r_{\text{h}}$  (and thus the half-mass radius under the assumption that mass follows light) is larger and therefore less difficult to retrieve from the data. For practical purposes, it is therefore useful to assume

$$r_{\text{c}} \propto r_{\text{h}} \quad (11)$$

and

$$\rho_0 \propto \frac{M}{r_h^3}, \quad (12)$$

where  $M$  is the mass of the stellar system. The King profile (King 1962) with its three independent parameters (core radius, tidal radius and central density), is thereby simplified to a density profile with only two independent parameters (half-mass radius and mass). The underlying assumptions are not necessarily true, and indeed, not fulfilled for GCs in the Milky Way since McLaughlin (2000) finds that more luminous GCs tend to be more concentrated. However, regarding the conclusions on how the presence of bright LMXBs is connected to the optical properties of GCs in the Virgo cluster, these assumptions are unproblematic. Using the same concentration for all GCs in their sample Sivakoff et al. (2007) find that they essentially come to the same results as Jordán et al. (2004), who use an individual estimate for the concentration of each GC in their sample.

When dealing with UCDs, replacing  $r_c$  with  $r_h$  is even advantageous. The time-scale on which the NSs gather at the centre of the UCD is given as

$$t_{\text{seg}} = \frac{\bar{m}}{m_{\text{ns}}} t_{\text{cc}}, \quad (13)$$

where  $\bar{m} \approx 0.5 M_\odot$  is the mean mass of stars,  $m_{\text{ns}} \approx 1.35 M_\odot$  is the mass of neutron stars and  $t_{\text{cc}}$  is the core-collapse time of the UCD without the NSs (Spitzer 1987; Banerjee et al. 2010). If a Plummer sphere (Plummer 1911) is used as an approximation for the density profile of a stellar system,  $t_{\text{cc}} \approx 15 t_{\text{rh}}$  holds (Baumgardt et al. 2002). With  $t_{\text{rh}}$  being of the order of a Hubble time for UCDs, Equation (13) implies that the distribution of NSs in UCDs still follows the initial distribution of their progenitors. The volume relevant for the formation of LMXBs in a UCD is therefore better measured by  $r_h$  than by  $r_c$ , provided its stellar population did not *form* mass-segregated. This is because  $r_h$  represents the size of the whole UCD, whereas  $r_c$  represents the size of its centre.

Thus, using Equations (11) and (12), Equation (10) can be transformed into

$$\Gamma_h \propto \frac{M^2}{r_h^3 \sigma}. \quad (14)$$

If the stellar system is also in virial equilibrium,

$$\sigma \propto \rho_0^{0.5} r_h \propto \frac{M^{0.5}}{r_h^{0.5}} \quad (15)$$

holds. In this case,

$$\Gamma_h \propto \frac{M^{1.5}}{r_h^{2.5}} \quad (16)$$

follows from Equations (14) and (15). In contrast to Equation (8), Equation (16) has only two variables ( $M, r_h$ ) instead of four ( $n_s, n_{\text{ns}}, M, r_c$ ).

A further variable can be eliminated by replacing individual values for  $r_h$  by luminosity-dependent estimates for  $r_h$ , such as Equations (6) and (7), and noting that the same SRMF for all stellar systems in question implies  $M \propto L_V$  for them. This leads to

$$\bar{\Gamma}_h \propto \frac{L_V^{1.5}}{\bar{r}_h^{2.5}}, \quad (17)$$

or, more explicitly by using Equations (6), and (7), respectively,

$$\log_{10}(\bar{\Gamma}_h) = 1.5 \log_{10} \left( \frac{L_V}{10^6 L_\odot} \right) + A \quad (18)$$

for GCs (i.e.  $L_V < 10^6 L_\odot$ ), and

$$\log_{10}(\bar{\Gamma}_h) = -1.190 \log_{10} \left( \frac{L_V}{10^6 L_\odot} \right) + A \quad (19)$$

for UCDs (i.e.  $L_V \geq 10^6 L_\odot$ ). The constant  $A$  is the same in Equations (18) and (19). Note that the transition between Equations (18) and (19) is continuous due to the continuity of  $\bar{r}_h$  at  $L_V = 10^6 L_\odot$ .

### 3.2.3. Detecting a variable SRMF with LMXBs

For investigating how  $\Gamma_h$  depends on the IMF, it is useful to consider the ratio between  $\Gamma_h$  as a function of  $\alpha_3$  and the  $\Gamma_h$  implied by some reference IMF. This has the advantage that factors, which do not depend on the IMF, cancel. The reference IMF is the canonical IMF in this paper; a choice that is motivated with the lack of dynamical evolution in UCDs (cf. Section 3.1). Using Equation (12) thus leads to

$$\frac{\Gamma_h(\alpha_3)}{\Gamma_h(\alpha_3 = 2.3)} = \frac{n_{\text{ns}}(\alpha_3)}{n_{\text{ns}}(\alpha_3 = 2.3)} \sqrt{\frac{M(\alpha_3 = 2.3)}{M(\alpha_3)}}, \quad (20)$$

if it also assumed that the IMF varies only for stars with  $m > m_{\text{to}}$ , so that also  $n_s$  is constant. By this last assumption, the luminosity of the UCDs, which is given by observations, stays constant when the IMF of the UCDs is varied. The right side of Equation (20) can be calculated if the IMF is specified. In particular,

$$\frac{n_{\text{ns}}(\alpha_3)}{n_{\text{ns}}(\alpha_3 = 2.3)} = \frac{\int_{8 \text{ M}_{\odot}}^{m_{\text{max}^*}} \xi(m) dm}{\int_{8 \text{ M}_{\odot}}^{m_{\text{max}^*}} \xi_{\text{can}}(m) dm}, \quad (21)$$

and

$$\frac{M(\alpha_3 = 2.3)}{M(\alpha_3)} = \frac{\int_{0.1 \text{ M}_{\odot}}^{m_{\text{max}^*}} m_{\text{rem}}(m) \xi_{\text{can}}(m) dm}{\int_{0.1 \text{ M}_{\odot}}^{m_{\text{max}^*}} m_{\text{rem}}(m) \xi(m) dm}, \quad (22)$$

where the IMF is normalised using Equation (2),  $\xi_{\text{can}}$  is the canonical IMF and  $m_{\text{rem}}(m)$  is given by Equation (4). Thus, Equation (20) quantifies how  $\Gamma_h$  changes in a stellar system (normalized with  $\Gamma_h$  for the canonical IMF) if the number of dark remnants and therefore the mass of the stellar system are changed, while its characteristic radius and the number of stars are kept constant.

A difficulty is that  $\Gamma_h$  of a stellar system cannot be measured directly. However, the actual  $\Gamma_h$  of a GC or a UCD scales with the rate at which LMXBs are created (see Sec. 3.2.1), which is proportional to the probability  $P$  to form an LMXB above a certain brightness limit in a given time. If a sample of GCs or UCDs in a certain luminosity interval is given, a useful estimator for the average  $P$  of these GCs or UCDs is the fraction  $f_{\text{LMXB}}$  of them that have an LMXB above the brightness limit defined by the sensitivity of a given set of observations. Thus,

$$f_{\text{LMXB}} \propto P \propto \Gamma_h^{\gamma}, \quad (23)$$

where the exponent  $\gamma$  accounts for the claims that the LMXB-frequency in GCs and UCDs may not be directly proportional to  $\Gamma$  or  $\Gamma_h$ , but to some power of  $\Gamma$  or  $\Gamma_h$  (cf. Jordán et al. 2004; Sivakoff et al. 2007).

If the SRMF of UCDs is indeed independent of luminosity, the  $f_{\text{LMXB}}$  of UCDs in different  $L_V$  intervals should all roughly coincide with the prediction from Equation (19) for an appropriate choice of the constant  $A$ . If however the  $f_{\text{LMXB}}$  of at least one  $L_V$  interval is inconsistent with Equation (19) for any choice of  $A$ , then this would be

evidence for the SRMF changing with the luminosity of the UCDs. This would imply that the IMF of the UCDs changes with luminosity, since the SRMF of UCDs is solely determined by stellar evolution, i.e. a process that does not depend on the size of the system (see Section 3.1). Note that the actual value of  $A$  in Equations (18) and (19) has no implications for the physical properties of the observed stellar systems: For a given sample of GCs and UCDs,  $A$  depends on the detection limit for an X-ray source or an arbitrarily chosen brightness limit above the detection limit.

### 3.2.4. Data on the LMXB-frequency in GCs and UCDs

In order to search for a dependency of the IMF in UCDs on their luminosity, we use data published in the upper left panel of figure (6) in Sivakoff et al. (2007). These data provide the fraction of globular clusters and UCDs,  $f_{\text{LMXB}}$ , hosting an LMXB in a given total  $z$ -band magnitude interval.

The results of Sivakoff et al. (2007) were obtained by combining two sets of data.

First, HST images of 11 elliptical galaxies in the Virgo Cluster were used, see Table 1 in Sivakoff et al. (2007). Ten of them are the brightest galaxies observed in the course of the ACS Virgo Cluster Survey (Côté et al. 2004). The eleventh one (NGC 4697) is a similarly bright galaxy that was observed by Sivakoff et al. (2007) with nearly the same observational setup as in the ACS Virgo Cluster Survey. Using the obtained images, a large number of accompanying GCs and UCDs was identified around each of these galaxies.

Second, Sivakoff et al. (2007) used archival Chandra Observatory X-ray observations of the same galaxies. The setup for the X-ray observations varied widely from galaxy to galaxy, see Table 2 in Sivakoff et al. (2007), which could in principle be problematic.

Sivakoff et al. (2007) find however that the global properties of GCs and UCDs which contain a LMXB are largely unaffected by the varying detection limits for X-ray sources. Also note that the LMXB-frequencies in GCs are well explained by the encounter rates in them (see Section 3.3), despite the different detection limits for X-ray sources. This suggests that the encounter rate



is indeed a good measure for the rate at which LMXBs of any X-ray luminosity are created. We therefore assume that a large number of GCs and UCDs with an X-ray source is indeed an indicator for a large number of dark remnants in them.

The size of the  $z$ -band magnitude intervals in Sivakoff et al. (2007) is chosen such that each of them contains 27 GCs or UCDs with a detected LMXB. This corresponds to a total of at least 100 GCs or UCDs in each of these intervals, since  $f_{\text{LMXB}} \lesssim 0.2$  in all of them. Thus,  $f_{\text{LMXB}}$  can be taken as a reliable estimator for the average  $P$  to form an LMXB in a GC or a UCD in a given  $z$ -band magnitude interval.

For comparing the data on the LMXBs in GCs and UCDs from Sivakoff et al. (2007) to the prediction for the LMXB-frequency in GCs and UCDs formulated in Equations (18) and (19),  $z$ -band magnitudes have to be converted into  $L_V$ . For this purpose,  $z$ -band luminosities are calculated from  $z$ -band magnitudes with

$$L_z = 10^{-0.4(M_z - 4.51)} L_{\odot,z}, \quad (24)$$

where  $M_z$  is the absolute  $z$ -band magnitude and  $L_z$  is  $z$ -band luminosity in Solar units (cf. Equation 1 in Sivakoff et al. 2007). Now note that the  $z$ -band  $M/L$  ratio of GCs in the Virgo-cluster are all close to  $\approx 1.5 M_{\odot}/L_{\odot,z}$  (Sivakoff et al. 2007), which is essentially identical to the average  $V$ -band  $M/L$  ratio of the GCs in the Milky Way in Solar units (McLaughlin 2000). This implies that  $z$ -band and  $V$ -band luminosities of GCs are approximately identical in Solar units. We therefore assume  $L_V/L_{\odot,V} = L_z/L_{\odot,z}$  in this paper.

The data from figure (6) in Sivakoff et al. (2007) is shown in Figure 4 with the  $z$ -band magnitude intervals from Sivakoff et al. (2007) converted into  $L_V$  intervals. Three of these intervals are at luminosities  $L_V > 10^6 L_{\odot}$ , so that the objects in them are UCDs (cf. Section 3.1). As the size of the intervals is chosen such that each of them contains 27 objects with an LMXB, 81 UCDs with an LMXB are considered here. The total number of UCDs in the sample from Sivakoff et al. (2007) is about 400, as can be calculated from  $f_{\text{LMXB}}$  in the according intervals.

For practical purposes, it is useful not to discuss individual values for the  $f_{\text{LMXB}}$  of UCDs, but to replace them by a continuous function  $\bar{P}(L_V)$ .

This function is obtained by performing a least-squares fit of a linear function to the values for  $f_{\text{LMXB}}$  in the  $L_V$  intervals with the UCDs, leading to

$$\log_{10}(\bar{P}) = a \log_{10}(L_V) + b, \quad (25)$$

where the best fitting parameters  $a$  and  $b$  are given in Tab. (1).  $\bar{P}$  can be interpreted as an estimate for the average probability for UCDs with a given  $L_V$  to host a LMXB brighter than the detection limit. For a meaningful comparison between  $\bar{P}$  and  $\bar{\Gamma}_h$  at different values for  $L_V$ ,  $A$  needs to be gauged. This is done by imposing that  $\bar{P}(L_V) = \bar{\Gamma}_h(L_V)$  for  $L_V = 10^6 L_{\odot,V}$ . The motivation for choosing this condition to fix  $A$  is that the stellar populations of systems with this luminosity should be nearly unaffected by dynamical evolution (cf. Section 3.1), while their  $M/L$ -ratios suggest that their IMF is canonical, in contrast to even more luminous stellar systems (cf. Dabringhausen et al. 2009).

If the rate at which LMXBs are produced in GCs and UCDs is proportional to some power  $\gamma$  of the encounter rate in them, leading to  $\bar{P}(L_V) \propto \bar{\Gamma}_h^{\gamma}$  (cf. Equations 23 and 25), Equation (20) can be transformed into

$$\frac{\bar{P}(L_V)^{\frac{1}{\gamma}}}{\bar{\Gamma}_h(L_V)} = \frac{n_{\text{ns}}(\alpha_3)}{n_{\text{ns}}(\alpha_3 = 2.3)} \sqrt{\frac{M(\alpha_3 = 2.3)}{M(\alpha_3)}}. \quad (26)$$

The left side of Equation (26) is then expressed in terms of observable properties of UCDs and the right side only depends on  $\alpha_3$  as a free parameter once  $m_{\text{tr}}$  is given. Equation (26) can therefore be used to estimate the dependency of the IMF of the UCDs as a function of their observed  $L_V$ . Since  $A$  is chosen such that  $\bar{P}(L_V)/\bar{\Gamma}_h(L_V) = 1$  for stellar systems that are assumed to have formed with the canonical IMF,  $\bar{P}(L_V)/\bar{\Gamma}_h(L_V) > 1$  implies a top-heavy IMF and  $\bar{P}(L_V)/\bar{\Gamma}_h(L_V) < 1$  implies a bottom-heavy IMF.

### 3.3. Results

In order to test for an LMXB-excess and thus a top-heavy IMF in UCDs from the observational data from Sivakoff et al. (2007) we now compare with theoretically expected LMXB-frequencies.

The dynamical formation of LMXBs depends on the density of both dark remnants and low-mass stars (Equation 8). In denser star clusters,

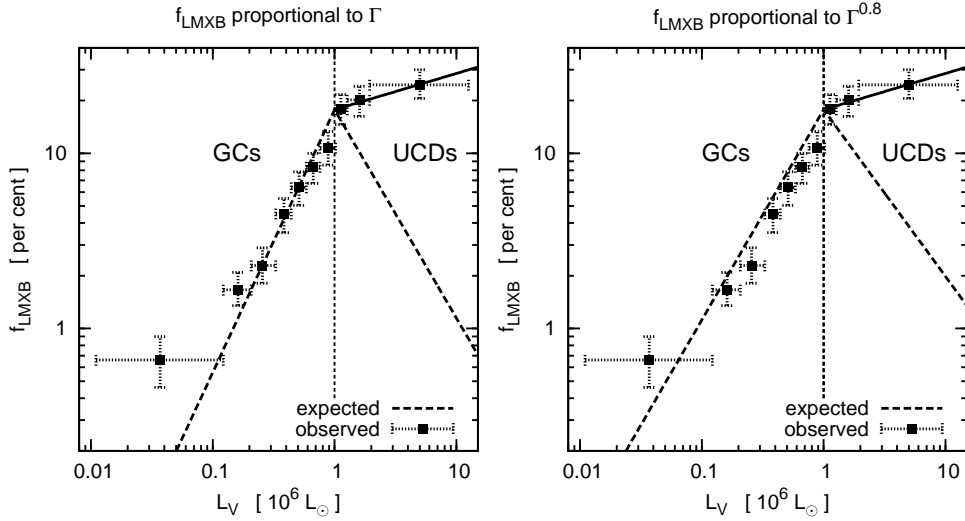


Fig. 4.— The observed LMXB-frequency of GCs and UCDs in comparison to expected frequencies if the IMF was canonical. Plotted are the observed frequencies (squares) of GCs ( $L_V < 10^6 L_{\odot,V}$ ) and UCDs ( $L_V \geq 10^6 L_{\odot,V}$ ) with LMXBs,  $f_{\text{LMXB}}$ , in the Virgo galaxy cluster as a function of the V-band luminosity,  $L_V$ . Each data point contains 27 objects showing the LMXB signal. The data points are identical with the data points in the upper left panel of figure (6) in Sivakoff et al. (2007), except for a rescaling of  $z$ -band magnitudes to  $V$ -band luminosities. The three brightest data are based on  $\approx 400$  UCDs, i.e.  $\approx 135$  UCDs per bin. The dashed line shows the theoretically expected LMXB-frequency for an invariant canonical IMF with index  $\alpha_3 = 2.3$  assuming  $f_{\text{LMXB}} \propto \bar{\Gamma}_h$  (left panel) and  $f_{\text{LMXB}} \propto \bar{\Gamma}_h^{0.8}$  (right panel). In either case, the theoretically expected LMXB-frequency is significantly too low for UCDs, while for GCs the theoretically expected LMXB-frequency matches the observed LMXB-frequency. The solid line is a fit through the UCD-regime (above  $10^6 L_{\odot,V}$ ). From it is derived the variation with luminosity of the IMF index  $\alpha_3$  such that this new model, based on a variable IMF, accounts for the observed  $f_{\text{LMXB}}$  for  $L_V > 10^6 L_{\odot,V}$ .

close encounters are more frequent and the formation of an LMXB is more likely. GCs have a common half-mass radius of a few parsec independent of their luminosity and their stellar mass is on average proportional to their luminosity (McLaughlin 2000). It therefore follows from Equation (18) that LMXBs should be hosted predominantly in high-mass GCs if their SRMF does not depend on their stellar mass. The dashed line in Figure 4 shows the theoretically expected LMXB frequency for a constant IMF calculated with Equations (18) and (19) with  $A$  chosen such that these equations reproduce the observed LMXB frequency at  $L_V = 10^6 L_{\odot}$ . The theoretical prediction then matches the observations in the GC regime (i.e.  $L_V < 10^6 L_{\odot}$ ), in agreement with earlier studies on LMXBs in GCs (Jordán et al. 2005; Peacock et al. 2010).

At  $L_V \approx 10^6 L_{\odot}$ , the transition luminosity

from GCs to UCDs, both kinds of stellar systems have the same half-mass radius (see Section 3.1). However, unlike GCs, UCDs show a luminosity-radius relation such that they become less dense with increasing luminosity (cf. figure 4 in Dabringhausen et al. 2008). Consequently, Equation (19) predicts that the capture rate of late-type stars by dark remnants and thus the expected LMXB frequency decreases rapidly with increasing  $L_V$ -band luminosity if the SRMF is constant. Note that a constant SRMF in UCDs implies a constant IMF in them due to the lack of dynamical evolution in UCDs (see Section 3.1).

In Figure 4, the prediction from Equation (19) for the LMXB frequency in UCDs with a constant SRMF is shown by the dashed line in the according luminosity range, where  $A$  is chosen such that Equation (19) reproduces the observed LMXB frequency at  $L_V = 10^6 L_{\odot}$ . Two cases are consid-

ered, namely  $f_{\text{LMXB}} \propto \Gamma_{\text{h}}$  and  $f_{\text{LMXB}} \propto \Gamma_{\text{h}}^{0.8}$ . The second case is closer to the dependency between  $f_{\text{LMXB}}$  and  $\Gamma_{\text{h}}$  reported by Sivakoff et al. (2007). The agreement between the theoretical prediction and the observed frequency of LMXBs is in either case good for GCs. However,  $f_{\text{LMXB}} \propto \Gamma_{\text{h}}^{0.8}$  seems indeed a better fit to the data than  $f_{\text{LMXB}} \propto \Gamma_{\text{h}}$ . Note that Maccarone & Peacock (2011) find  $\Gamma \propto \Gamma_{\text{h}}^{0.8}$  on average for GCs in the Milky Way, which essentially means that the typical ratio between  $\Gamma$  and  $\Gamma_{\text{h}}$  depends for these GCs on their mass. This is probably a consequence of the more massive GCs in the MW being more concentrated than the less massive ones (McLaughlin 2000; cf Section 3.2.2), and likely to be the case for the GCs in the Virgo cluster as well.

For UCDs however, the observed LMXB-frequency strongly deviates from the theoretical prediction for a constant SRMF. It is observed that  $25 \pm 5$  per cent of the UCDs with  $L_V \approx 5 \times 10^6 L_{\odot,V}$  have a bright LMXB, while Equation (19) suggests a LMXB frequency of about 2 per cent at this luminosity for  $f_{\text{LMXB}} \propto \Gamma_{\text{h}}$  and a LMXB frequency of about 3 per cent for  $f_{\text{LMXB}} \propto \Gamma_{\text{h}}^{0.8}$ . Thus, the expected fraction of LMXBs hosting UCDs is up to  $\approx 10$  times smaller than observed if all UCDs had the same IMF.

This discrepancy between the data and the model with an invariant (canonical) IMF and the data is highly significant. This cannot be explained with more dark remnants remaining bound to UCDs due to higher escape velocities. This is because the escape velocity from massive GCs is much higher than the escape velocity from light GCs, since the characteristic radii of GCs do not change with mass, but the encounter rate is nevertheless sufficient for quantifying which fraction of them has a bright LMXB.

The situation is more complicated with the finding that redder GCs and UCDs have more LMXBs than the blue ones, while brighter objects (i.e. the UCDs in particular) tend to be redder than the less luminous ones (Mieske et al. 2006). Taking color as an indicator for metallicity leads to the interpretation that the LMXB-frequency in GCs and UCDs does not only depend on  $\Gamma$  or  $\Gamma_{\text{h}}$  but also on metallicity (Jordán et al. 2004; Sivakoff et al. 2007). Note that an increase of metallicity with luminosity and therefore mass of GCs is consistent with theoretical modeling,

according to which more massive star clusters retain more processed (i.e. metal-enriched) gas which is turned into subsequent stellar populations (Tenorio-Tagle et al. 2003).

Using metallicity (i.e. color) as a second parameter besides  $\Gamma_{\text{h}}$  indeed allows a more precise modeling of the probability to find a LMXB in a given GC or UCD than when  $\Gamma_{\text{h}}$  is assumed to be the sole parameter determining the probability to find a LMXB in that GC or UCD (Sivakoff et al. 2007). The dependency of that probability is however nevertheless almost linear to the encounter rate, while the dependency on the metallicity is much weaker (Jordán et al. 2004; Sivakoff et al. 2007). This may explain why the fraction of GCs with a LMXB is apparently already well explained if only the encounter rate in the GCs is considered (see Figure 4) despite the color-luminosity relation for GCs in the Virgo cluster (cf. Mieske et al. 2006). It is thereby unlikely that the drastic discrepancy between the observed LMXB-frequency in UCDs and the theoretical prediction based on the encounter rate can be explained by an unaccounted metallicity effect, even though the color-luminosity dependency may be somewhat more pronounced for UCDs than for GCs (Mieske et al. 2010).

The conclusion is that the large number of LMXBs in UCDs is best explained by a large number of dark remnants as a consequence of a top-heavy IMF in UCDs (and not as a consequence of different escape velocities or metallicities).

For an invariant IMF the theoretical LMXB frequency is highest at a luminosity of  $L_V \approx 10^6 L_{\odot,V}$ , because in these systems the present-day stellar density has a maximum and close encounters are most frequent (Figure 4 in Dabringhausen et al. 2008). If the very dense star formation conditions are responsible for a top-heavy IMF then, on first sight, the smallest IMF index  $\alpha_3$  is expected in systems with  $L_V \approx 10^6 L_{\odot,V}$  and not in the most luminous UCDs. However, in systems with a top-heavy IMF stellar feedback is strongly enhanced and rapid gas expulsion leads to an expansion of the UCDs (Dabringhausen et al. 2010). The UCDs revirialise after a few dynamical time scales ( $\lesssim 100$  Myr) and undergo no further size evolution. Thus, their present day stellar density is the dynamically relevant quantity for producing the LMXB population.

We now determine by what amount the dark remnant content in UCDs has to be increased to get the theoretical LMXB-frequency into agreement with the observed values. For this, Equation (26) with  $\gamma = 1$  and  $\gamma = 0.8$  is used. This equation has  $\alpha_3$  and  $m_{\text{tr}}$  as parameters (Equation 1). In this paper,  $m_{\text{tr}} = 1 \text{ M}_\odot$  and  $m_{\text{tr}} = 5 \text{ M}_\odot$ , so that the influence of the in principle quite arbitrary choice of  $m_{\text{tr}}$  is tested. Note that with  $m_{\text{tr}} = 1 \text{ M}_\odot$ , Equation (1) describes the family of IMFs that were considered in Dabringhausen et al. (2009). For either choice of  $m_{\text{tr}}$ , the canonical IMF (Kroupa 2001, 2002) corresponds to  $\alpha_3 = 2.3$  and a smaller value of  $\alpha_3$  increases the fraction of high-mass stars and subsequent dark remnants. The  $\alpha_3$  that can explain the discrepancy between  $\overline{P}(L_V)$  (i.e. the function describing the observed LMXB frequency in UCDs) and  $\overline{\Gamma}_h(L_V)$  (i.e. the theoretical expectation for the LMXB frequency in UCDs if their IMF was canonical) at a given  $L_V$  can be found by numerically solving Equation (26) for  $\alpha_3$  with a given value for  $m_{\text{tr}}$ .

The  $L_V$  dependence of  $\alpha_3$  required to bring the model into agreement with the UCD data is plotted as the solid line in Figure 5 for  $m_{\text{tr}} = 1 \text{ M}_\odot$  and in Fig (6) for  $m_{\text{tr}} = 5 \text{ M}_\odot$ . In either case, the most massive UCDs must have an extremely top-heavy IMF in order to explain their LMXB-excess. The higher  $m_{\text{tr}}$  is, the more exotic the IMF of UCDs must be in order to explain the number of LMXBs in them. For a given value for  $m_{\text{tr}}$ , it is on the other hand only of minor importance whether  $P(L_V)$  is proportional to  $\overline{\Gamma}_h$  or proportional to  $\overline{\Gamma}_h^{0.8}$ .

For  $m_{\text{tr}} = 1 \text{ M}_\odot$ , the independent analysis in this paper leads the same top-heavy IMF as derived from the UCD mass-to-light ratios (Dabringhausen et al. 2009), shown as the dotted line in Figure 5. Such a comparison is not meaningful for  $m_{\text{tr}} = 5 \text{ M}_\odot$ , since the shape thereby assumed for the IMF is different from the IMF considered in Dabringhausen et al. (2009).

The most likely relations between  $\alpha_3$  and  $\log_{10}(L_V)$  shown in Figures 5 and 6 are remarkably close to a linear function,

$$\overline{\alpha}_3 = c \log_{10}(L_V) + d. \quad (27)$$

The best fitting parameters  $c$  and  $d$  have been determined from a least-squares fit to 48 sample

values calculated from Equation (26). These are shown Table 1. Probably the best model for the IMF in UCDs is calculated when  $f_{\text{LMXB}} \propto \Gamma_h^{0.8}$  and  $m_{\text{tr}} = 1 \text{ M}_\odot$  are assumed. This is because observations suggest a less-than-linear dependency of  $f_{\text{LMXB}}$  on the encounter rate (Jordán et al. 2004; Sivakoff et al. 2007) and assuming  $m_{\text{tr}} > 1 \text{ M}_\odot$  implies even more extreme deviations from the canonical IMF in high-mass UCDs while the IMF is remarkably invariant in open star clusters (Kroupa 2001).

Figure 4 suggests that the value of  $f_{\text{LMXB}}$  for the most luminous UCDs is of central importance for estimating the slope of  $\overline{P}(L_V)$  (Equation 25) and thus for the  $\alpha_3$  calculated from Equation (26). This is because of the distance of these data points to the other data points, which is due to the fact that the corresponding  $L_V$  interval is large. In order to estimate an uncertainty to the dependency of  $\alpha_3$  on  $L_V$ , we changed the value of  $f_{\text{LMXB}}$  for the most luminous UCDs ( $L_V \gtrsim 2 \times 10^6 L_\odot$ ) by 3 times its uncertainty.  $\overline{P}(L_V)$  was then recalculated with this new value and used in Equation (26). The resulting limits on the dependency of  $\alpha_3$  on  $L_V$  are indicated by the limits to the gray area in Figures 5 and 6. Also the limits of the gray areas are parametrized with linear functions, which are listed in Table 1.

The uncertainty of the upper mass limit for stars,  $m_{\text{max}*}$ , has little effect on the results summarized in Table 1. This is illustrated with Figure 7, where the dependency between  $L_V$  and  $\alpha_3$  calculated from Equation (26) is shown for  $m_{\text{max}*} = 150 \text{ M}_\odot$  (Weidner & Kroupa 2004; Oey & Clarke 2005) and for  $m_{\text{max}*} = 300 \text{ M}_\odot$  (Crowther et al. 2010). The two functions are almost identical.

#### 4. The supernova rate in Arp 220

A top-heavy IMF in UCDs can theoretically be understood if UCDs formed as very massive star clusters that were internally heated by infrared radiation that was trapped inside a molecular cloud massive enough to form a UCD-type star cluster (Murray 2009), or if UCDs formed from molecular clouds that were heated by highly energetic cosmic rays originating from numerous type-II supernovae surrounding those molecular clouds (Papadopoulos 2010; cf. Section 1). Both sce-

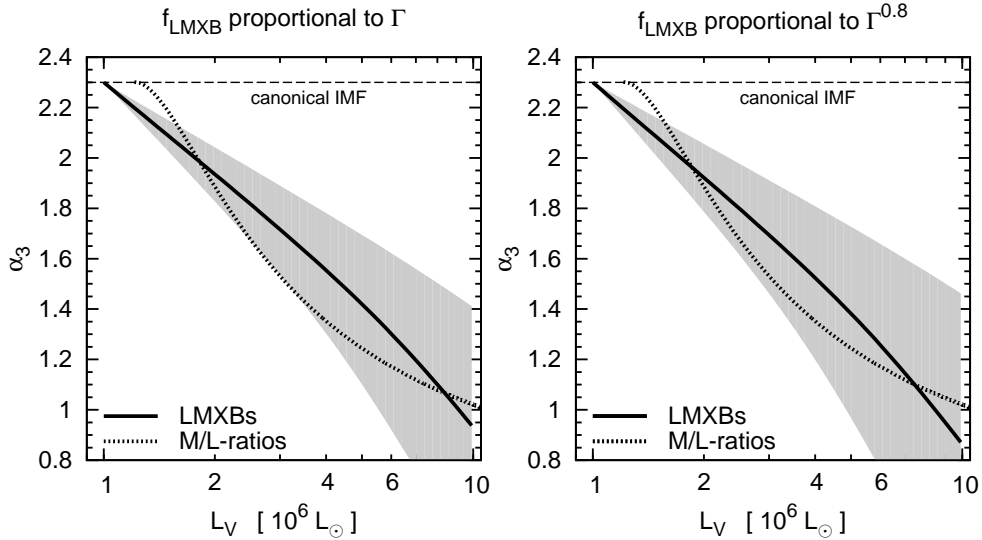


Fig. 5.— The IMF in UCDs for  $m_{\text{tr}} = 1 M_{\odot}$ . Plotted is the high-mass IMF index,  $\alpha_3$ , as a function of the V-band luminosity of the UCDs,  $L_V$  for  $f_{\text{LMXB}} \propto \Gamma_h$  leading to  $P(L_V) \propto \bar{\Gamma}_h$  (left panel) and for  $f_{\text{LMXB}} \propto \Gamma_h^{0.8}$  leading to  $P(L_V) \propto \bar{\Gamma}_h^{0.8}$  (right panel). The solid line shows the most likely high-mass index required to increase the dark remnant content in UCDs in order to match to observed LMXB-frequency (derived from the solid line in Figure 4). The grey shaded area marks an estimate for the  $3\sigma$  region. The horizontal long dashed line marks the canonical IMF with  $\alpha_3 = 2.3$ . The dotted line shows the independently calculated high-mass IMF index obtained from the observed mass-to-light ratios of UCDs (Dabringhausen et al. 2009). Simple-to-use fitting relations for the variation of  $\alpha_3$  with  $L_V$  can be found in Tab. (1).

narios imply that UCDs are formed during star-bursts, either because of the link between the formation of the most massive star-clusters and high star formation rates (Weidner et al. 2004), or because the cosmic-ray field would only then be intense enough for effective heating of the molecular clouds. Note that likely progenitors of UCDs have actually been observed in star-bursts (Fellhauer & Kroupa 2002).

Ultra-luminous infra-red galaxies (ULIRGs) are believed to be galaxies with star-bursting regions (Condon et al. 1991). They are thus systems where UCDs are probably forming. If this notion is correct and the IMF in UCDs is top-heavy, the ULIRGs as a whole should have more massive stars than expected for an invariant, canonical IMF. As a consequence, the rate of type II supernovae is expected to be higher.

In the following, we test the hypothesis of a top-heavy IMF in ULIRGs. For this reason, we quantify how the type-II supernova rate (SNR) in a star burst is connected to the star formation

in it. Based on this, theoretical predictions for the SNR of Arp 220, which is one of the closest ULIRGs (Lonsdale et al. 2006), are calculated and compared to observations of this stellar system.

The type-II supernova rate (SNR) observed in a stellar system depends on its IMF as well as on its star formation history (SFH), i.e. how the star formation rate in the stellar system has changed with time, because these quantities determine the numbers and ages of stars in given mass intervals. If star formation begins at a time  $t_0$ , only stars above a time-dependent mass-limit  $m_{\text{low}}$  can have completed their evolution at a time  $t > t_0$ . For stars evolving into SNe, this mass can be approximated (Dabringhausen et al. 2010) by

$$\frac{m_{\text{low}}}{M_{\odot}} = 74.6 \left( \frac{t - t_0}{\text{Myr}} - 2.59 \right)^{-0.63}. \quad (28)$$

Note that no stars evolve to type-II supernovae (SNe), if  $t - t_0 \leq 2.59$  Myr.

Now consider a time interval  $[t, t + \Delta t]$  and stars in a mass interval  $[m, m + \Delta m]$ , where  $m \geq m_{\text{low}}$ .

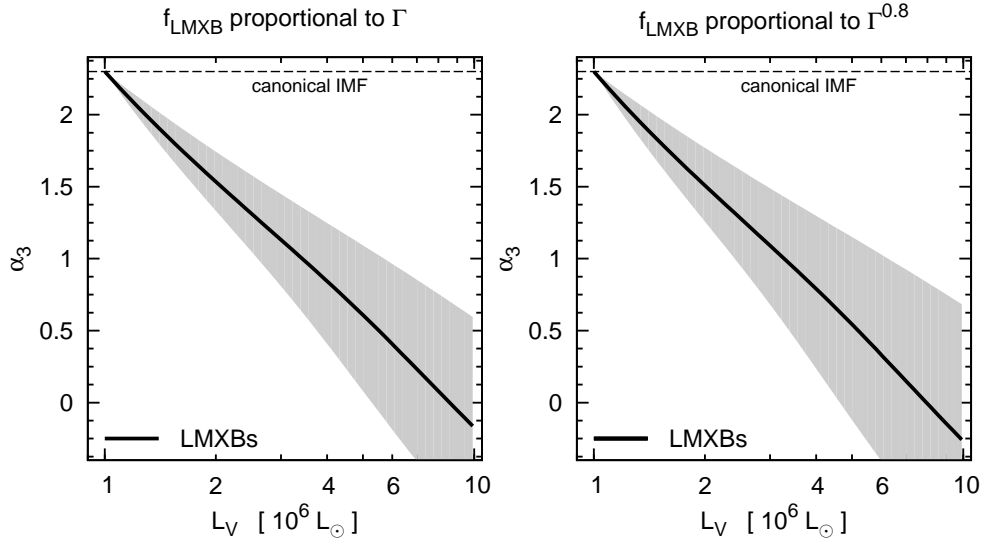


Fig. 6.— The IMF in UCDs for  $m_{\text{tr}} = 5 M_{\odot}$ , otherwise as Figure 5.

If the SFR was constant for all  $t \geq t_0$ , the number of stars evolving into SNe in the given mass interval during the time  $\Delta t$  is equal to the number of new stars that are formed in the same mass interval. Thus,

$$\frac{\Delta \text{SNR}}{\text{yr}^{-1}} = \frac{\text{SFR}}{M_{\odot} \text{ yr}^{-1}} \int_m^{m+\Delta m} \xi(m) dm \quad (29)$$

in this case, where  $\xi(m)$  is assumed to be given by Equation (1) with the normalization defined by Equation (3). This normalization keeps the total mass of the stars which are formed per unit time constant.

If  $\Delta t$  is small compared to the time scale on which  $m_{\text{low}}$  changes, the number of all stars that evolve during  $\Delta t$  can be approximated as

$$\frac{\text{SNR}}{\text{yr}^{-1}} \approx \frac{\text{SFR}}{M_{\odot} \text{ yr}^{-1}} \int_{m_{\text{low}}}^{m_{\text{max}}} \xi(m) dm. \quad (30)$$

Note that the SFR in Equations (29) and (30) should be considered an average value over a time-scale  $t - t_0$ . Variations of the SFR on much shorter time-scales are of no importance here.

The SFR of a ultra-luminous infra-red galaxy (ULIRG) can be estimated as

$$\frac{\text{SFR}}{M_{\odot} \text{ yr}^{-1}} = \frac{L_{\text{FIR}}}{5.8 \times 10^9 L_{\odot}}, \quad (31)$$

where  $L_{\text{FIR}}$  is the far infra-red (FIR) luminosity of the ULIRG (Kennicutt 1998).

One of the nearest ULIRGs is Arp 220. Using  $L_{\text{FIR}} = 1.41 \times 10^{12} L_{\odot}$  for Arp 220 (Sanders et al. 2003), Equation (31) implies a SFR of  $\approx 240 M_{\odot} \text{ yr}^{-1}$  for that galaxy. The SNe in Arp 220 have been observed in a central region with a diameter of  $\approx 1$  kpc, from where about 40 per cent of its FIR luminosity originates (Soifer et al. 1999). Equation (31) thus implies a SFR of  $\approx 100 M_{\odot} \text{ yr}^{-1}$  if only this part of Arp 220 is considered. Note that this SFR is consistent with the SFR that has been suggested for a forming UCD if UCDs form on a timescale of approximately 1 Myr (Dabringhausen et al. 2009). Also note that the observed SN in Arp 220 do not seem to distributed evenly over the central part of Arp 220, but to be concentrated in two knots which have a radius  $\approx 50$  pc each (Lonsdale et al. 2006) (i.e. the size of a UCD). This implies that indeed a major part of the star formation in the central part of Arp 220 takes place within these two knots. This would imply projected star formation densities of a few  $10^{-3} M_{\odot} \text{ yr}^{-1} \text{ pc}^{-2}$  in the knots.

SNRs calculated from Equation (30) for a constant SFR of  $100 M_{\odot} \text{ yr}^{-1}$  are shown as functions of the high-mass slope of the IMF in Figure 8. The two curves correspond to different times at which the star burst was initialized, but the expected number of SN per year (i.e. the SNR) is low in any case. The number of SN that *actually* occur

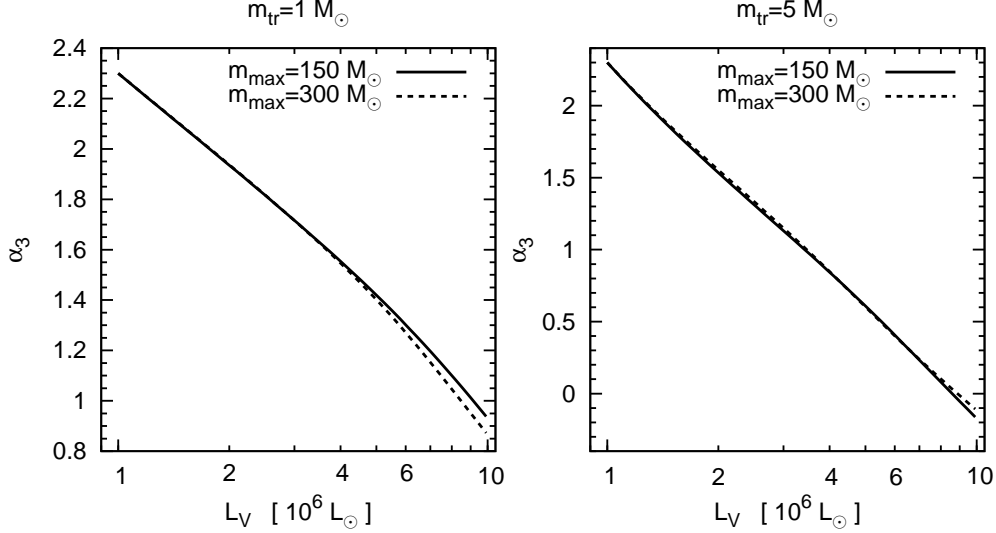


Fig. 7.— The high-mass IMF slope,  $\alpha_3$ , as a function of  $V$ -band luminosity for different upper mass limits of the IMF,  $m_{\max*}$  assuming  $m_{\text{tr}} = 1 M_{\odot}$  (left panel) or  $m_{\text{tr}} = 5 M_{\odot}$  (right panel). The solutions,  $\alpha_3(L_V)$ , are calculated from Equation (26) with  $\gamma = 1$ , i.e. under the assumption that  $f_{\text{LMB}} \propto \Gamma_h$ . Assuming  $\gamma = 0.8$  leads however qualitatively to the same results as assuming  $\gamma = 1$  (c.f. Figures 5 and 6). The solid line corresponds in both panels to  $m_{\max*} = 150 M_{\odot}$  and is thus identical with the solid line in Figure 5, and Figure 6, respectively. The dashed lines corresponds to  $m_{\max*} = 300 M_{\odot}$ .

within one year can therefore differ substantially from the calculated SNR, as the frequency of SN over such a time span obeys low-number statistics. Thus, the probability for a certain number of SN to happen within one year is quantified by the Poisson distribution function.

Now consider the case that the star-burst in Arp 220 already lasts for more than 40 Myr. This implies  $m_{\text{low}} = 8 M_{\odot}$ , so that the number of SNII per year is maximized for the given SFR. The expectation value for the SNII-rate is then about one per year if the IMF was canonical (i.e.  $\alpha_3 = 2.3$ ), but about two per year for a top-heavy IMF with  $1 \lesssim \alpha_3 \lesssim 2$ , where the SN-rate is only a weak function of  $\alpha_3$  (cf. Figure 8). Thus, the probability to actually observe four new SNII in a given year (Lonsdale et al. 2006) is then about two per cent if the IMF is canonical, but about 12 per cent for  $1 \lesssim \alpha_3 \lesssim 2$ .

A more elaborate discussion of the SNII rate in Arp 220 is obtained by taking into account that stars in a galaxy form in star-clusters of different masses, since  $m_{\max}$  of the IMF depends on the mass of the star-cluster for low-mass star-

clusters. This implies that the integrated galactic IMF (IGIMF) of all star-clusters in Arp 220 combined is not equal to the IMF in its star-clusters.

This IGIMF is given by

$$\xi_{\text{IGIMF}}(m) = \int_{M_{\text{ecl},\min}}^{M_{\text{ecl},\max}(\text{SFR})} \xi(m \leq m_{\max}(M_{\text{ecl}})) \times \xi_{\text{ecl}}(M_{\text{ecl}}) dM_{\text{ecl}}, \quad (32)$$

where  $m$  is the initial stellar mass,  $M_{\text{ecl}}$  is the initial stellar mass of a star cluster,  $M_{\text{ecl},\min}$  is the minimum mass of newly formed star-clusters,  $M_{\text{ecl},\max}(\text{SFR})$  is the SFR-dependent maximum mass of newly formed star-clusters,  $\xi(m)$  is the IMF and  $\xi_{\text{ecl}}(M_{\text{ecl}})$  is the star-cluster mass function (Weidner & Kroupa 2005; Weidner et al. 2011). The IGIMF can be parametrized by a multi-power law,

$$\xi_{\text{IGIMF}}(m) = k k_i m^{-\alpha_i}, \quad (33)$$

with

$$\begin{aligned} \alpha_1 &= 1.3, & 0.1 \leq \frac{m}{M_{\odot}} < 0.5, \\ \alpha_2 &= 2.3, & 0.5 \leq \frac{m}{M_{\odot}} < 1, \end{aligned}$$

Table 1: The best fitting parameters for linear fits to  $P$  and  $\alpha_3$  for different models. The different cases (most likely case, upper limit, lower limit) listed here for every model correspond to different values of  $P$  for the UCDs with the highest masses (cf. Sec 3.3). Probably the best model for the IMF in UCDs is calculated when  $f_{\text{LMXB}} \propto \Gamma_h^{0.8}$  and  $m_{\text{tr}} = 1 \text{ M}_\odot$  are assumed. This is because observations suggest a less-than-linear dependency of  $f_{\text{LMXB}}$  on the encounter rate (Jordán et al. 2004; Sivakoff et al. 2007) and assuming  $m_{\text{tr}} > 1 \text{ M}_\odot$  implies even more extreme deviations from the canonical IMF in high-mass UCDs while the IMF is remarkably invariant in open star clusters (Kroupa 2001). The parameters describing the IMF according to this model are shown in bold face in this table.

model	$\log_{10}(\overline{P}) = a \log_{10}(L_V) + b$		$\overline{\alpha_3} = c \log_{10}(L_V) + d$	
	$a$	$b$	$c$	$d$
$f_{\text{LMXB}} \propto \Gamma_h, m_{\text{tr}} = 1 \text{ M}_\odot$ , most likely case	0.207	1.249	-1.337	2.332
$f_{\text{LMXB}} \propto \Gamma_h, m_{\text{tr}} = 1 \text{ M}_\odot$ , upper limit	0.615	1.201	-1.878	2.375
$f_{\text{LMXB}} \propto \Gamma_h, m_{\text{tr}} = 1 \text{ M}_\odot$ , lower limit	-0.202	1.298	-0.884	2.396
$f_{\text{LMXB}} \propto \Gamma_h^{0.8}, m_{\text{tr}} = 1 \text{ M}_\odot$ , most likely case	0.207	1.249	- <b>1.402</b>	<b>2.337</b>
$f_{\text{LMXB}} \propto \Gamma_h^{0.8}, m_{\text{tr}} = 1 \text{ M}_\odot$ , upper limit	0.615	1.201	- <b>2.089</b>	<b>2.391</b>
$f_{\text{LMXB}} \propto \Gamma_h^{0.8}, m_{\text{tr}} = 1 \text{ M}_\odot$ , lower limit	-0.202	1.298	- <b>0.861</b>	<b>2.304</b>
$f_{\text{LMXB}} \propto \Gamma_h, m_{\text{tr}} = 5 \text{ M}_\odot$ , most likely case	0.207	1.249	-2.415	2.275
$f_{\text{LMXB}} \propto \Gamma_h, m_{\text{tr}} = 5 \text{ M}_\odot$ , upper limit	0.615	1.201	-3.169	2.289
$f_{\text{LMXB}} \propto \Gamma_h, m_{\text{tr}} = 5 \text{ M}_\odot$ , lower limit	-0.202	1.298	-1.679	2.263
$f_{\text{LMXB}} \propto \Gamma_h^{0.8}, m_{\text{tr}} = 5 \text{ M}_\odot$ , most likely case	0.207	1.249	-2.512	2.277
$f_{\text{LMXB}} \propto \Gamma_h^{0.8}, m_{\text{tr}} = 5 \text{ M}_\odot$ , upper limit	0.615	1.201	-3.442	2.290
$f_{\text{LMXB}} \propto \Gamma_h^{0.8}, m_{\text{tr}} = 5 \text{ M}_\odot$ , lower limit	-0.202	1.298	-1.594	2.263

$$\alpha_{\text{IGIMF}} \in \mathbb{R}, \quad 1 \leq \frac{m}{\text{M}_\odot} \leq m_{\text{max*}},$$

where the factors  $k_i$  ensure that the IGIMF is continuous where the power changes and  $k$  is a normalization constant.  $\xi_{\text{IGIMF}}(m)$  equals 0 if  $m < 0.1 \text{ M}_\odot$  or  $m > m_{\text{max*}}$ , where  $m_{\text{max*}}$  is the maximum stellar mass. Thus, the IGIMF defined here is equal to the IMF defined by Equation (1), except for the high-mass slope and the upper mass limit.

The case of a canonical IMF in all star-clusters, i.e.  $\alpha_3 = 2.3$ , implies (Weidner & Kroupa 2005)  $\alpha_{\text{IGIMF}} \gtrsim 3$ . The expectation value for the number of SNII per year would then be  $\lesssim 0.2$  per year. On the other hand,  $\alpha_{\text{IGIMF}} \lesssim 2$  is possible, if a varying IMF that becomes more top-heavy with star-cluster mass is considered (Weidner et al. 2011; Kroupa et al. 2011). This implies that the probability to actually observe four new SNII in a given year (Lonsdale et al. 2006) is essentially zero if the IMF is canonical in all star-clusters, but it can still be about 10 per cent if the IMF becomes top-heavy in massive UCD-type star-clusters.

The remnants produced by SNII are neutron stars and black holes. The SNII-rates thereby

are an indicator for how many mergers of such remnants can be detected by searching for gravitational waves. Comparing the SN-rate for  $\alpha_{\text{IGIMF}} = 3$  to the SN-rate for  $\alpha_{\text{IGIMF}} = 2$  thus suggests that about an order of magnitude more of such events may be expected if the IMF in massive star-clusters is not canonical, but top-heavy. Thus, the hitherto predicted detection rate of about 30 mergers of dark remnants per year (Banerjee et al. 2010) for the upcoming adLIGO-experiment could be too low by an order of magnitude, as an invariant IMF has been used for this estimate.

Further evidence for a top-heavy IMF in star-bursting galaxies is found by Anderson et al. (2011) in Arp 299. They study numbers of different types of supernovae in Arp 299 and conclude from the mass of the appropriate progenitor stars that the IMF is probably top-heavy in that system. Thus, Anderson et al. (2011) qualitatively come to the same conclusion for Arp 299 as we did for Arp 220, while their method is different.



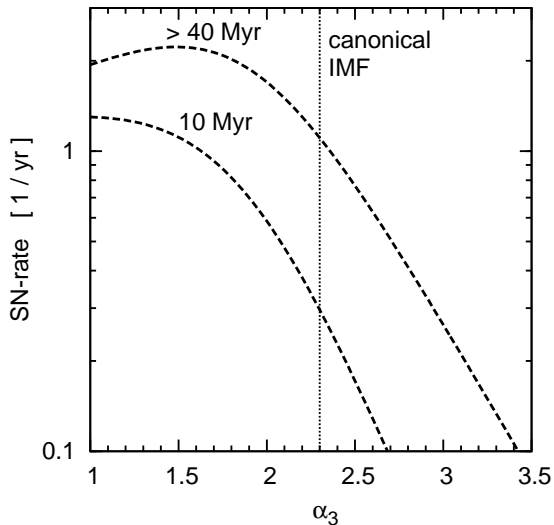


Fig. 8.— The SN-rate in the center of Arp 220. The SN-rates are functions of the slope of the IMF above a stellar mass of  $1 M_{\odot}$ ,  $\alpha_3$ , but also depend on the length of the star burst (which is indicated above the corresponding curve). They do not exceed  $\approx 1 \text{ SN yr}^{-1}$  for the canonical IMF (whose high-mass slope is marked by the dotted vertical line), or  $\approx 2 \text{ SN yr}^{-1}$  for a top-heavy IMF.

## 5. Star formation densities and the IMF

A top-heavy IMF in UCDs is in-line with different studies concluding a top-heavy IMF in high-redshift star forming galaxies (van Dokkum 2008; Loewenstein 2006). Contrary to this, a recent spectroscopic study of two low-redshift very massive elliptical galaxies suggests a hitherto unseen large population of low-mass stars (van Dokkum & Conroy 2010), which has been predicted as a possible consequence of cooling flows on massive ellipticals (Kroupa & Gilmore 1994). It is on the other hand unlikely that the majority of the UCDs formed in potential wells deeps enough to cause cooling flows.

Also note that the current stellar densities suggest that the star-formation densities (SFDs), i.e. the SFR per volume, of UCDs were very different from the SFDs of elliptical galaxies. Consider for instance an exemplar present-day UCD with  $M = 10^7 M_{\odot}$  and  $r_h = 10 \text{ pc}$  and an exemplar present-day elliptical galaxy with  $M = 10^{12} M_{\odot}$  and  $r_h = 10^4 \text{ pc}$ . These values can be consid-

ered representative for typical UCDs and massive elliptical galaxies, respectively (cf. figure 4 in Misgeld & Hilker 2011). Star formation is thought to have proceeded quickly in UCDs and massive elliptical galaxies, so that the stellar population of the exemplar UCD may have formed within  $10^7 \text{ yr}$  (Dabringhausen et al. 2009) and the stellar population of the exemplar elliptical galaxy may have formed within  $10^9 \text{ yr}$  (Thomas et al. 2005). This leads to a SFR of  $1 M_{\odot} \text{ yr}^{-1}$  for the exemplar UCD and to a SFR of  $10^3 M_{\odot} \text{ yr}^{-1}$  for the exemplar elliptical galaxy. The SFD can be estimated by dividing the SFR by  $r_h^3$ , leading to a SFD of  $10^{-3} M_{\odot} \text{ yr}^{-1} \text{ pc}^{-3}$  for the exemplar UCD and a SFD of  $10^{-9} M_{\odot} \text{ yr}^{-1} \text{ pc}^{-3}$  for the exemplar elliptical galaxy. However, according to Dabringhausen et al. (2010) UCDs must have been even more compact when they formed ( $r_h \approx 1 \text{ pc}$ ), since the mass loss following star formation with a top-heavy IMF must have expanded them to their present-day radii. With the masses of UCDs being  $10^6 M_{\odot} \lesssim M \lesssim 10^8 M_{\odot}$ , their SFRs ranged from  $0.1 M_{\odot} \text{ yr}^{-1}$  to  $10 M_{\odot} \text{ yr}^{-1}$  if they formed within 10 Myr. An initial  $r_h$  of 1 pc thereby implies SFDs ranging from  $0.1 M_{\odot} \text{ yr}^{-1} \text{ pc}^{-3}$  to  $10 M_{\odot} \text{ yr}^{-1} \text{ pc}^{-3}$ . Thus, the SFDs of UCDs can easily be higher by six to ten orders of magnitude than the SFDs of massive elliptical galaxies. Massive ellipticals can therefore not serve as a proxy for the stellar population in UCDs.

It is therefore perhaps the SFD that determines whether the IMF in some region of space becomes top-heavy, and not the overall SFR in a forming stellar system. This is actually consistent with models why the IMF may become top-heavy: Dabringhausen et al. (2010) argue that the central densities in forming UCDs were so high ( $\rho > 10^5 M_{\odot} \text{ pc}^{-3}$ ) that collisions and perhaps mergers between pre-stellar cores were important in them, in contrast to less massive stellar systems. Likewise, if the heating of molecular clouds by cosmic rays is the process by which the IMF becomes top-heavy (Papadopoulos 2010), it is again not the number, but the number *density* of the surrounding massive stars that makes heating of the molecular cloud effective.

## 6. Conclusion

The dynamical mass-to-light ratios of ultra compact dwarf galaxies (UCDs) are surprisingly high (Hasegan et al. 2005; Dabringhausen et al. 2008; Mieske et al. 2008). This finding was explained by Dabringhausen et al. (2009) with an IMF that has more massive stars than the canonical IMF deduced by Kroupa (2001) from resolved stellar populations in the Milky Way. The high mass-to-light ratio of UCDs is then a consequence of a large population of dark remnants (i.e. neutron stars and black holes) in them.

These dark remnants become visible as X-ray sources if they accrete matter from a low-mass companion star. The rate at which low-mass X-ray binaries (LMXBs) are formed in globular clusters and UCDs scales with the number density of dark remnants (see Section 3.2.1). Data on the fraction of UCDs that harbour a bright X-ray source (Sivakoff et al. 2007) can therefore be used to confirm the presence of a large population of dark remnants in UCDs by a method that does not rely on the fact that dark remnants only increase the mass of a UCD, but not its luminosity. It is shown in this paper that LMXBs in UCDs are indeed up to 10 times more frequent than expected for an invariant, canonical IMF. The overabundance of LMXBs is used to quantify the dependence of the high-mass IMF-slope,  $\alpha_3$ , on the luminosity of UCDs. This function is essentially equal to the dependence between the luminosity of the UCDs and their  $\alpha_3$  suggested in Dabringhausen et al. (2009) based on the mass-to-light ratios of UCDs (see Section 3.3). Note that the  $L_V$  of present-day GCs and UCDs is just one of many properties of such systems. Dependencies of  $\alpha_3$  on their initial mass, initial density and their metallicity are therefore discussed in Marks et al. (2012).

UCDs can be understood as the most massive star-clusters which only form at extremely high galaxy-wide star formation rates (SFRs) (Weidner & Kroupa 2004). Alternatively, UCDs could form by the merger of gravitationally bound systems of star clusters as they are observed in interacting galaxies (Fellhauer & Kroupa 2002). In either case, the formation of UCDs would be connected to star-bursts. Given that ultra-luminous infra-red galaxies (ULIRGs) are interpreted as

galaxies with star-bursting regions (Condon et al. 1991), they should show indications of a top-heavy IMF as a consequence. The nearest ULIRG is Arp 220. We show that the observed rate of type II supernovae in this ULIRG is indeed highly improbable if the IMF is invariant, but not if the IMF is top-heavy (see Section 4).

There are thus three mutually consistent arguments for a top-heavy IMF in UCDs or more generally star-bursting systems. Together with the evidence for the formation of UCDs being connected to star bursts, these arguments imply that the IMF becomes top-heavy in star-bursts (cf. Weidner et al. 2011). This finding stands in contrast to the prevalent notion that the IMF is invariant (Kroupa 2001, 2002; Bastian et al. 2010; Kroupa et al. 2011) and thereby has important implications. For instance, estimates of the SFR of a galaxy based on observations that are sensitive only to high-mass stars and the assumption of an invariant IMF (like Equation 31) are too high if the IMF actually is top-heavy. Consequently, estimates for the time scale on which the population of low-mass star in that galaxy is built up until the gas of the galaxy is depleted become too short. Also the chemical evolution of galaxies is different if the IMF in them can become top-heavy, since the nuclear reactions that occur in a star mainly depend on its mass. This has implications on their content of metals and planetary systems (Ghezzi et al. 2010). Furthermore, as more dark remnants are formed if the IMF is top-heavy, more dark-remnant mergers and thus gravitational-wave emitters should be detected in this case. Finally, the dynamical evolution of star clusters critically depends on the shape of the IMF (Dabringhausen et al. 2010).

## Acknowledgments

J.D acknowledges support through DFG-grant KR1635/13 and thanks ESO for financial support via a grant from the Director General Discretionary Fund in 2009. The authors wish to thank Tom Maccarone for some useful comments.

## REFERENCES

Anderson, J. P., Haberman, S. M., & James, P. A. 2011, MNRAS, 416, 567

- Banerjee, S., Baumgardt, H., & Kroupa, P. 2010, *MNRAS*, 402, 371
- Banerjee, S., Kroupa, P., & Oh, S. 2011, ArXiv e-prints
- Bastian, N., Covey, K. R., & Meyer, M. R. 2010, *ARA&A*, 48, 339
- Baumgardt, H., Hut, P., & Heggie, D. C. 2002, *MNRAS*, 336, 1069
- Baumgardt, H. & Mieske, S. 2008, *MNRAS*, 391, 942
- Brown, G. E., Heger, A., Langer, N., et al. 2001, *New A*, 6, 457
- Casares, J. 2007, in *IAU Symposium*, Vol. 238, IAU Symposium, ed. V. Karas & G. Matt, 3–12
- Chilingarian, I. V., Cayatte, V., & Bergond, G. 2008, *MNRAS*, 390, 906
- Condon, J. J., Huang, Z., Yin, Q. F., & Thuan, T. X. 1991, *ApJ*, 378, 65
- Côté, P., Blakeslee, J. P., Ferrarese, L., et al. 2004, *ApJS*, 153, 223
- Crowther, P. A., Schnurr, O., Hirschi, R., et al. 2010, *MNRAS*, 408, 731
- Dabringhausen, J., Fellhauer, M., & Kroupa, P. 2010, *MNRAS*, 403, 1054
- Dabringhausen, J., Hilker, M., & Kroupa, P. 2008, *MNRAS*, 386, 864
- Dabringhausen, J., Kroupa, P., & Baumgardt, H. 2009, *MNRAS*, 394, 1529
- Drinkwater, M. J., Gregg, M. D., Hilker, M., et al. 2003, *Nature*, 423, 519
- Evstigneeva, E. A., Gregg, M. D., Drinkwater, M. J., & Hilker, M. 2007, *AJ*, 133, 1722
- Fellhauer, M. & Kroupa, P. 2002, *MNRAS*, 330, 642
- Forbes, D. A. & Kroupa, P. 2011, *Publications of the Astronomical Society of Australia*, 28, 77
- Ghezzi, L., Cunha, K., Smith, V. V., et al. 2010, *ApJ*, 720, 1290
- Gilmore, G., Wilkinson, M. I., Wyse, R. F. G., et al. 2007, *ApJ*, 663, 948
- Goerdt, T., Moore, B., Kazantzidis, S., et al. 2008, *MNRAS*, 385, 2136
- Hasegan, M., Jordán, A., Côté, P., et al. 2005, *ApJ*, 627, 203
- Hilker, M., Baumgardt, H., Infante, L., et al. 2007, *A&A*, 463, 119
- Hilker, M., Infante, L., Vieira, G., Kissler-Patig, M., & Richtler, T. 1999, *A&AS*, 134, 75
- Ivanova, N., Heinke, C. O., Rasio, F. A., Belczynski, K., & Fregeau, J. M. 2008, *MNRAS*, 386, 553
- Jordán, A., Côté, P., Blakeslee, J. P., et al. 2005, *ApJ*, 634, 1002
- Jordán, A., Côté, P., Ferrarese, L., et al. 2004, *ApJ*, 613, 279
- Kennicutt, Jr., R. C. 1998, *ApJ*, 498, 541
- King, I. 1962, *AJ*, 67, 471
- Kroupa, P. 2001, *MNRAS*, 322, 231
- Kroupa, P. 2002, *Sci.*, 295, 82
- Kroupa, P. & Gilmore, G. F. 1994, *MNRAS*, 269, 655
- Kroupa, P., Weidner, C., Pflamm-Altenburg, J., et al. 2011, ArXiv e-prints
- Kumar, B., Sagar, R., & Melnick, J. 2008, *MNRAS*, 386, 1380
- Loewenstein, M. 2006, *ApJ*, 648, 230
- Lonsdale, C. J., Diamond, P. J., Thrall, H., Smith, H. E., & Lonsdale, C. J. 2006, *ApJ*, 647, 185
- Maccarone, T. J. & Peacock, M. B. 2011, *MNRAS*, 415, 1875
- Marks, M., Kroupa, P., Dabringhausen, J., Pawlowski, M. 2012, ArXiv e-prints
- McLaughlin, D. E. 2000, *ApJ*, 539, 618
- Mieske, S., Hilker, M., Jordán, A., et al. 2008, *A&A*, 487, 921

- Mieske, S., Jordán, A., Côté, P., et al. 2006, *ApJ*, 653, 193
- Mieske, S., Jordán, A., Côté, P., et al. 2010, *ApJ*, 710, 1672
- Misgeld, I. & Hilker, M. 2011, *MNRAS*, 414, 3699
- Murray, N. 2009, *ApJ*, 691, 946
- Oey, M. S. & Clarke, C. J. 2005, *ApJ*, 620, 43
- Papadopoulos, P. P. 2010, *ApJ*, 720, 226
- Peacock, M. B., Maccarone, T. J., Kundu, A., & Zepf, S. E. 2010, *MNRAS*, 407, 2611
- Plummer, H. C. 1911, *MNRAS*, 71, 460
- Sanders, D. B., Mazzarella, J. M., Kim, D., Surace, J. A., & Soifer, B. T. 2003, *AJ*, 126, 1607
- Sivakoff, G. R., Jordán, A., Sarazin, C. L., et al. 2007, *ApJ*, 660, 1246
- Soifer, B. T., Neugebauer, G., Matthews, K., et al. 1999, *ApJ*, 513, 207
- Spitzer, L. 1987, *Dynamical evolution of globular clusters*, ed. Spitzer, L.
- Tenorio-Tagle, G., Palouš, J., Silich, S., Medina-Tanco, G. A., & Muñoz-Tuñón, C. 2003, *A&A*, 411, 397
- Thomas, D., Maraston, C., Bender, R., & Mendes de Oliveira, C. 2005, *ApJ*, 621, 673
- van Dokkum, P. G. 2008, *ApJ*, 674, 29
- van Dokkum, P. G. & Conroy, C. 2010, *Nature*, 468, 940
- Verbunt, F. 2003, in *Astronomical Society of the Pacific Conference Series*, Vol. 296, *New Horizons in Globular Cluster Astronomy*, ed. G. Piotto, G. Meylan, S. G. Djorgovski, & M. Riello, 245–+
- Verbunt, F. & Hut, P. 1987, in *IAU Symposium*, Vol. 125, *The Origin and Evolution of Neutron Stars*, ed. D. J. Helfand & J.-H. Huang, 187–197
- Weidner, C. & Kroupa, P. 2004, *MNRAS*, 348, 187
- Weidner, C. & Kroupa, P. 2005, *ApJ*, 625, 754
- Weidner, C. & Kroupa, P. 2006, *MNRAS*, 365, 1333
- Weidner, C., Kroupa, P., & Bonnell, I. A. D. 2010, *MNRAS*, 401, 275
- Weidner, C., Kroupa, P., & Larsen, S. S. 2004, *MNRAS*, 350, 1503
- Weidner, C., Kroupa, P., & Pflamm-Altenburg, J. 2011, *MNRAS*, 979